Stages in the Interaction of Deuterium Atoms with Amorphous Hydrogenated Carbon Films: Isotope Exchange, Soft-Layer Formation and Steady-State Erosion

G. S. Oehrlein[(1)], T. Schwarz-Selinger, K. Schmid, M. Schlüter and W. Jacob
Max-Planck-Institut für Plasmaphysik, EURATOM Association, Boltzmannstr. 2, D-85748 Garching, Germany

ABSTRACT

We report studies of the interactions of quantified deuterium (hydrogen) atom beams with hard amorphous hydrogenated carbon films at a substrate temperature of ~330 K in an ultrahigh-vacuum (UHV) chamber. The modification/erosion of a-C:H (a-C:D) films was monitored in-situ by ellipsometry in real-time. By interpreting the ellipsometric information and combining it with measurements of the absolute D areal density changes of the a-C:H (a-C:D) films by ion beam analysis as a function of D (H) atom fluence, we are able to distinguish three sequential stages of D interaction with hard a-C:H films. The first stage is replacement of bonded hydrogen by deuterium up to an areal density of $\sim 5\times10^{15}$ D cm^{-2} to a depth of ~1.4 nm from the surface. This phase is complete after a deuterium fluence of $\approx 2\times10^{18}$ cm^{-2}. The effective cross section for isotopic exchange of H with D atoms for the a-C:H layer is found to be $\sigma = 2.0\times10^{-18}$ cm^2, and is close to the cross section for H abstraction from a carbon surface. This may indicate that H abstraction by D from the a-C:H surface is the rate limiting step for isotope exchange in this situation. Hydrogen replacement is followed by creation of additional C-D bonds in the near-surface region and increases the D areal density by about 2.5×10^{15} D cm^{-2}. By ellipsometry this process can be observed as the formation of a soft a-C:D layer on top of the hard a-C:H bulk film, with the soft layer extending about 1.4 nm from the surface. This stage is complete after a deuterium fluence of about 2×10^{19} cm^{-2}. Subsequently, steady-state erosion of the a-C:H film takes place. Here, a soft a-C:D layer with roughly constant thickness (~1.4 nm) remains on the hard a-C:H substrate and is dynamically reformed as the underlying hard a-C:H film becomes thinner. A similar sequence of processes takes place at a substrate temperature of 650 K, albeit at a much faster rate.

Published with JOURNAL OF APPLIED PHYSICS:
Received: 01 February 2010
Accepted for publication: 5 July 2010
Published online: 24 August 2010
J. Appl. Phys. **108**, 043307 (13pp) (2010).
doi: 10.1063/1.3474988

[1] Author to whom correspondence should be addressed; Work performed while on sabbatical leave from Department of Materials Science & Engineering and Institute for Research in Electronics and Applied Physics, University of Maryland, College Park, Maryland 20742, oehrlein@umd.edu.

I. Introduction.

The reactions of hydrogen atoms produced in gas discharges with carbon-based substrates are ubiquitous and have been of sustained interest. Hydrogen-carbon substrate interactions are important for hydrocarbon discharges employed for deposition of carbon films [1], diamond-like carbon films [2], carbon nanotubes and carbon nanofibers [3,4,5], graphene, growth of polymer like-films [6,7], along with H_2 plasma induced surface modifications and etching of carbon films, polymers and polymer-like materials [8,9,10,11,12,13]. The associated applications range from H_2 containing discharges used for carbon resist mask removal in semiconductor device fabrication [12], sterilization for medicine and food packaging [14], to the interaction of D/T plasma with carbon surfaces in thermonuclear fusion devices [15].

Often, hydrogen-carbon substrate interactions play a dominant role in outcomes of plasma-surface processes. For instance, final film properties during growth of amorphous hydrogenated carbon (a–C:H) films by plasma-based deposition processes depend strongly on substrate temperature [16], bombardment by energetic species, e.g. H ions, and interaction with neutral H atoms [16, 17]. Von Keudell and Jacob showed that interaction of low-energy hydrogen species with a–C:H films produces a modified layer at the surface which is characterized by high H content and low refractive index, typical of soft, polymer-like a–C:H films [16, 18]. Hydrogen atoms are thought to hydrogenate sp^2–hybridized carbon atoms at the carbon film surface and convert them to sp^3 species, thus increasing the H density at the surface. The sp^3–hybridized terminal groups are thought to be the precursors for the chemical erosion step [18,19].

The interaction of H atoms and H ions with graphite and other carbonaceous materials has also been a topic of long-standing interest in the thermonuclear fusion community and has recently been reviewed by Jacob and Roth [15]. Carbon erosion of plasma-facing carbon components in deuterium/tritium plasmas, e.g. in the divertor region of a thermonuclear fusion device, followed by redeposition of tritium-containing carbon layers can lead to significant tritium retention in fusion devices [20,21,22,23]. One important issue for the design of the International Thermonuclear Experimental Reactor (ITER) is the question if a carbon-based divertor is acceptable for this device, since safety-necessitated removal of redeposited tritium containing carbon layers may require unacceptably long cleaning times and reduce the useful plasma operating time of the reactor to an impractically low level [22]. The goal to improve the scientific understanding of the factors that control carbon erosion and redeposition in D/T-based fusion devices has lead to significant research efforts aimed at establishing the mechanisms of carbon erosion in hydrogen or deuterium plasma environments [19, 23,24]. For the understanding of plasma-surface interactions, elucidation of details on the interaction mechanisms of both neutral atoms and ions with carbon layers is of interest.

In the present work, we studied the interaction of deuterium or hydrogen atom beams with hard a-C:H (a-C:D) films [25] at a substrate temperature of 330 K to clarify important stages of hydrogen-carbon interaction. Our results clearly show the existence of three distinct stages of deuterium-carbon layer interaction. These are hydrogen replacement by deuterium atoms in the near-surface region of the hydrocarbon film (uptake of $\sim 5\times10^{15}$ D cm^{-2}), followed by creation of additional C-D bonds ($\sim 2.5\times10^{15}$ D cm^{-2}) which establishes a soft a-C:D layer. Ellipsometric measurements and analysis show that the soft modified layer extends about 1.4 nm from the surface. Finally, steady-state erosion of the a-C:H film takes place, where a dynamic soft a-C:D layer with roughly constant thickness remains on the substrate.

A brief overview of this article is as follows: In **part II** we present the experimental procedures employed in this work. In **part III** we first report data on the change of the D areal densities with D atom fluence obtained by ion beam analysis (IBA). A description of the results of real-time ellipsometric measurements of an a-C:H layer during D atom and H atom exposures follows, along with detailed explanation of the ellipsometric multiple layer modeling used for the interpretation of the experimental data. We also present data on a-C:H erosion behavior using either D or H atom beams at a substrate temperature of 650 K. In **part IV** of the paper, we describe additional analysis of the IBA and ellipsometric data obtained during D atom exposures of a-C:H films**.** We conclude this section with a discussion of physical mechanisms that can explain the different erosion rates measured during D and H atom exposures of a-C:H layers. Conclusions are presented in **part V**.

II. Experimental.

Ultrahigh-Vacuum (UHV) Chamber for Deuterium And Hydrogen Exchange. The deuterium and hydrogen exchange experiments were performed in the ultrahigh-vacuum (UHV) chamber of the experiment MAJESTIX that contains multiple particle beams for interaction with a substrate and has been described in detail in Ref. [26]. The components of MAJESTIX employed in the present work are shown in Fig. 1. Deuterium or hydrogen atom beams were produced by thermal dissociation of D_2 or H_2 flowing through a resistively heated tungsten capillary (see Ref. [27] for a detailed description of the atom beam sources). The D_2 or H_2 flow to the inlet of the capillary was controlled by calibrated mass flow controllers. The experiments were conducted using the same pressure at the high pressure side of the capillary (0.5mbar). The pressure on the inlet of the capillary was measured using a capacitance manometer. The pressure in the UHV chamber during the experiments was measured by an ionization gauge. Plasma-deposited a-C:H (or a-C:D) films on Si substrates were exposed to defined H or D atom fluxes at various temperatures.

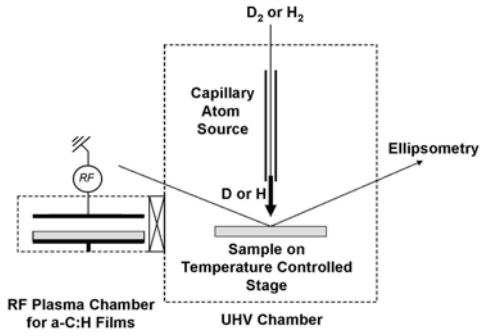

Fig. 1

Figure 1: *Schematic of components of the particle-beam experiment MAJESTIX used in this work. A tungsten capillary heated to 2200 K was used to produce D or H atoms from D_2 or H_2 gas flowing through the capillary. In-situ ellipsometry was employed for optical monitoring of the sample surface. Deposition of hard a-C:H layers on Si was performed in the sample preparation chamber, which also served as a load-lock of the UHV chamber*

The absolute D atom flux at the sample position was obtained by a flux calibration method described by Schwarz-Selinger et al. [27]. A hard a-C:H film was deposited in the sample preparation chamber of the UHV apparatus, and transferred in vacuum into the main chamber for erosion studies. The erosion rate of the hard a-C:H film is measured in-situ by ellipsometry at a sample temperature of 650 K. This corresponds to the temperature maximum of the chemical erosion yield. The erosion yield Y for these conditions is known from literature and amounts to $Y \sim 0.02 \pm 0.004$ [C atoms per impinging D atom] [27,28]. The thickness change measured by ellipsometry is converted to the number of eroded C atoms using the relationship established by Schwarz-Selinger et al. [25]. The D flux is finally obtained from the number of removed C atoms divided by the erosion yield. Using this procedure the atomic D flux at the sample position was determined to be 1.3×10^{15} D cm^{-2} s^{-1}. The absolute uncertainty of this flux value is determined by the uncertainty of the yield plus the general uncertainty of the reproducibility of operational parameters of the source which are estimated to be well below 10%. The relative error of the fluxes used in this study is only determined by the day-to-day reproducibility of the source. Since most operational parameters of the source were not changed during the course of these experiments, this relative uncertainty is estimated to be less than 5%. In contrast, the H atom flux from the source has not been calibrated and the erosion yield for H atoms has not been determined in prior work. The conductivity of the capillary exhibits a mass dependence, and the H_2 flow through the capillary is expected to be ~40 % greater than the D_2 flow if the same inlet pressure is used. Erosion rates for a-C:H films using D and H atom beams were measured at 650 K, and will be shown in section III.

The substrate temperature during the experiments is measured using two thermocouples. One thermocouple (TC) is pressed from the front against the a-C:H coated Si sample. The second TC is located on the backside of the Cu sample holder. During experiments without active heating of the sample holder, the Si sample temperature increased due to radiative heating from the capillary atom source from room temperature to a temperature of 330 ± 5 K. Although the sample temperature reading was stable during the D or H atom exposures, the actual temperature at the location where the D or H atoms struck may have been slightly higher.

Real-time *in situ* optical monitoring of changes in the near surface region of amorphous C layers being exposed to the atom beams was performed by single-wavelength ellipsometry at 632.8 nm. In section III, representative results of these measurements will be shown and their interpretation discussed.

a-C:H Films. The bulk of the deuterium exchange experiments were performed with a-C:H films deposited on 10 cm diameter single crystalline silicon wafers using a capacitively coupled plasma reactor pumped with a turbomolecular pump and equipped with an in-situ ellipsometry setup [29]. Either CH_4 or CD_4 were used for film deposition. Plasma was produced by feeding 13.56 MHz RF power to the wafer holder on which the Si substrates were located. Typical experimental conditions for the a-C:H (a-C:D) film deposition experiments were a gas pressure of 2 Pa, a total CH_4 (or CD_4) gas flow of 40 sccm, a RF power level of 26 W, and a selfbias voltage of -300 V. These conditions enabled deposition of hard a-C:H films with a refractive index of $n = 2.15$ and $k = 0.136$ at 632.8 nm. Most of the films produced in this fashion and employed in this work had a thickness of about 70 nm. Properties of a-C:H films deposited in a similar fashion have been described by Schwarz-Selinger et al. [25]. Additionally, we

prepared 20 nm thick a-C:D films on silicon using the same experimental conditions for complementary H and D atom exposures. The small thickness of the a-C:D films on silicon allowed film thickness to be determined by ellipsometry, but prevented accurate determination of film optical properties. We assumed that film properties, including the D/D+C ratio and H/H+C ratios of the films, were comparable. The overall consistency of the findings supports this assumption. After deposition, 2.5 cm by 2.5 cm pieces were cut from the Si wafers and introduced through the load-lock into the UHV chamber for the D or H atom beam interaction experiments.

As mentioned above, some a-C:H films were also deposited in the specimen preparation chamber of MAJESTIX and transferred under vacuum into the ultra-high vacuum chamber (see Fig. 1). This preparation chamber also served as a load-lock of the UHV chamber [26], and enabled sample introduction of a-C:H (or a-C:D) films on Si produced in the well-characterized RF deposition chamber described above.

Nuclear Reaction Analysis (NRA). The total deuterium areal density (D cm^{-2}) of treated and untreated carbon films was determined using nuclear reaction analysis employing the $D(^3He,p)^4He$ reaction. The measurement was performed at an incident ^3He ion energy of 690 keV. At this energy, the cross section [30] for this reaction is at its maximum and thus the measurement is most sensitive to the near surface D areal density. Since the penetration depth of the ^3He projectiles is larger than the film thickness of the samples used here (~70 nm and ~20 nm), NRA measures the deuterium content in the complete layer. The protons from the nuclear reaction were collected in a semiconductor surface barrier detector with opening angle of 0.15 sr. The detector was covered with a 12 μm mylar foil to stop scattered primary ^3He projectiles and ^4He particles from the nuclear reaction allowing only the protons from the nuclear reaction to enter the detector. Each of the spectra was measured with a He fluence of 5 μC which is a good compromise between counting statistics and minimizing sample changes due to particle-induced release of D during the measurement. Dedicated release measurements showed that for an analyzing dose of 5μC less than 10 % of the D was lost during the NRA measurement. Since this is of the same order of magnitude as the uncertainty of the target current measurement, the NRA data presented in this article were not corrected for particle-induced release. To convert the integral over the detected proton signal into a D areal density, the following calibration procedure was applied: Given the detector solid angle of 0.15 sr, the reaction cross section from [30] and the analyzing dose of 5 μC, SIMNRA (a program for the simulation of backscattering spectra for ion beam analysis [31]) was used to calculate the integral of the proton spectrum (Φ) corresponding to an areal density of 10^{15} D cm^{-2}. Using the so calculated $\Phi = 263$ counts / 10^{15} D cm^{-2} / 5 μC, the experimental proton spectra integrals were converted by dividing them by Φ, yielding the D areal densities in multiples of 10^{15} D cm^{-2}.

III. Experimental Results.

Changes in deuterium areal density as a function of D or H atom fluence. In Fig. 2 we show NRA data on the changes in deuterium areal density (D cm^{-2}) of hard a-C:H or a-C:D layers after exposure to D or H atoms at ~330 K versus exposure time for three different sets of experiments. The corresponding D atom fluence is shown on the top of the figure. Since a calibration of the H atom source in this system has not been performed, the actual H atom fluence corresponding to a given exposure time may be different from the D atom fluence shown. This will be discussed in more detail in section IV.

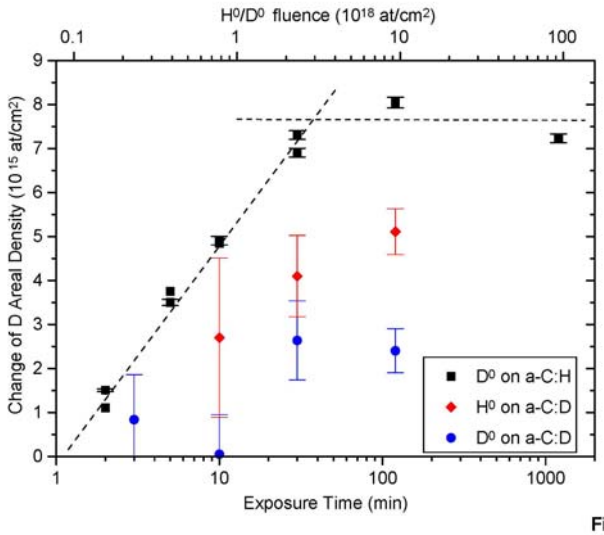

Fig. 2

Figure 2: *Deuterium areal density of hard a-C:H layers after exposure to D atoms at 330 K versus exposure time (bottom scale) or D atom fluence (top scale), respectively. In addition, the change in the D density of a-C:D layers exposed to either D or H atoms is shown. The fluence scale shown on the top is correct for D atoms. The actual H atom fluence corresponding to a given exposure time may be different.*

The different experiments for which results are presented are exposures of i) a-C:H films to D atoms, ii) a-C:D films to D atoms, and iii) a-C:D films to H atoms, respectively. When exposing a-C:H films to D atoms, we find that the total D areal density initially increases in an exponential fashion with time, and then slows down and saturates. The D saturation value of approximately 7.5×10^{15} D cm^{-2} is reached after an exposure time of about 40 to 100 min. For the experimental deuterium flux of 1.3×10^{15} D/cm^2 s this corresponds to a D fluence of about 3×10^{18} to 8×10^{18} D cm^{-2}.

The net change in deuterium areal density as a result of exposure of hard a-C:H layers to D atoms is explained by both isotopic substitution of H atoms in the near-surface region of the a-C:H layer (isotope exchange), and formation of extra C-D bonds, e.g. by deuteration of C-C bonds that may break and reform dynamically, but in the presence of D form extra C-D bonds. The NRA technique only provides information on the total D atom areal density change. We attempted to distinguish the contribution of isotopic substitution of H atoms by D relative to formation of extra C-D bonds to the overall D areal density change by performing

complementary sets of experiments. In these experiments we determined the change of the D areal density of a-C:D layers exposed to either D or H atom beams. The measured D areal density changes are also shown in Fig. 2. We would like to comment on the significant scatter in these data, and the fact that error bars are much larger than when exposing a-C:H films to D atoms. The relatively large uncertainty for these experiments is explained by the fact that a small change of the D areal density has to be determined relative to a large background of D atoms present in the 20 nm thick a-C:D layers. The estimated total D areal density in the 20 nm thick a-C:D film is about 8×10^{16} D cm^{-2} [25], i.e., it is about a factor of 30 higher than the amount of additionally incorporated D atoms. In contrast, when exposing a-C:H films to D atoms, the D background is negligible. The estimated D background from the natural abundance of D in H (0.015 % [32]) in the 70 nm thick a-C:H film is about 4×10^{13} D cm^{-2}. The background measurement by NRA yielded a value of $(2.8\pm0.5)\times10^{13}$ D cm^{-2}. Both values are less than 1 % of the measured D exchange. The plotted error bars in Fig. 2 correspond to the maximum and minimum values measured on different spots of the samples.

We assume that the change of the D areal density when exposing a-C:D films to D atoms provides information on the areal density of extra C-D bonds formed. Based on this, Fig. 2 shows that extra D atoms are incorporated at an areal density of $\sim2.5\times10^{15}$ D cm^{-2} after 120 min for our experimental conditions.

The loss of the D areal density of a-C:D layers exposed to H atoms provides information on the number of D atoms replaced by isotopic substitution. The data of Fig. 2 show that hydrogen replaces D atoms at a level of $\sim5\times10^{15}$ D cm^{-2} after 120 min H atom exposure. Again, large error bars are shown for the D areal density data obtained for H atom exposures of a-C:D films, and can be explained by the relatively small change in total D areal density caused by the replacement of D atoms by H atoms in the near-surface region. The D background present in the 20 nm thick a-C:D layers is in this case by a factor of 16 higher than the net change of the D areal density due to isotopic replacement of D by H atoms.

Consistent with expectations, Fig. 2 shows that the sum of the changes of D areal densities measured for experiments where a-C:D films were exposed for 120 min to D atoms or H atoms, respectively, equals the change of D areal density determined at saturation in the set of experiments were a-C:H films were exposed to D atoms, and provides the total incorporation of D in the a-C:H layers.

Real-time ellipsometry measurements at 330 K and interpretation. In Fig. 3 we present ellipsometry data (solid circles) obtained during deuteration of a hard a-C:H film at 330 K for a total exposure time of 20 h. Several key physical processes that take place at the surface of the sample will be introduced when describing Fig. 3. The identification of these processes is based on detailed comparisons of the measured ellipsometry data with optical modeling results that are shown in Figs. 4(a) and (b). The modeling procedures and the corresponding interpretation of the data will be explained when discussing Figs. 4(a) and (b).

Curve 1 in Fig. 3 (solid squares) shows model results of the Psi-Delta angles that correspond to the growth of a hard a–C:H film (n = 2.15, k = 0.136) on a Si substrate [25]. The point to point difference of the model curve corresponds to a thickness change of 0.1 nm. The actual a-C:H film thickness used in the experiment agrees with point *A* (location where the experimental data and the simulation intersect and which corresponds to the start of deuterium atom exposure) and equals 74 nm. As the hard a-C:H layer is exposed to the D atoms, the ellipsometric angles change with time and initially move along path 2 to point *B* which is reached after 180 min exposure time, and finally along 3 to point *C* (reached after 1200 min, and

corresponding to the end of the experiment). The movement from point *B* to point *C* takes place on a curve that is parallel to curve 1, but the movement is in opposite direction, and is interpreted as film erosion. The model trajectory shown in Fig. 3 that is parallel to arrow 3 (open squares) corresponds to the simulation of a hard a-C:H layer of varying thickness underneath a soft a-C:H layer of constant thickness (1.4 nm) and optical properties given by $n = 1.57$ and $k = 0$. The optical properties of the soft a-C:H layer are characteristic of hydrocarbon polymers [25,33]. The fact that the temporal behavior of the a-C:H layer over many hours can be described by an ellipsometric model involving a soft a-C:H overlayer of constant thickness over unmodified a-C:H strongly supports the thickness value and optical properties of the soft layer derived by the simulation of the steady-state erosion behavior. The temporal evolution of the a-C:H surface prior to the steady-state situation will be described in more detail below, and further supports the correctness of this model. We considered but rejected other possible surface modifications, e.g. surface roughening. Surface roughness typically increases with the amount of material removed (or deposited), as has been seen in other studies of D_2 plasma-based a-C:H film erosion [34] or plasma-polymer interactions by members of this group [35,36]. The behavior seen here is completely different. The required time scale of roughness introduction is also inconsistent with the current data, whereas the comparison of the temporal dependencies of soft a-C:H overlayer formation and D uptake measured by NRA are completely consistent.

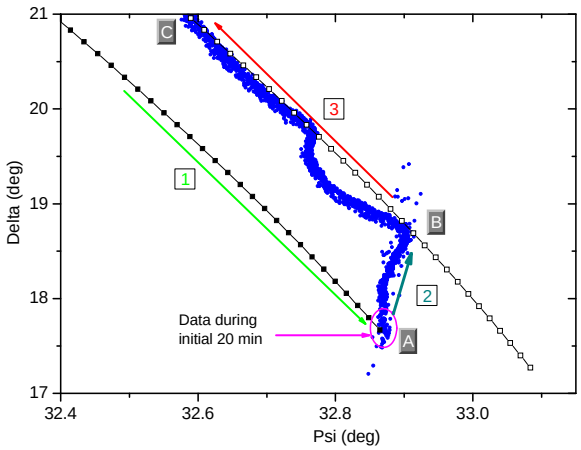

Figure 3: *Ellipsometry data obtained during deuteration of hard a-C:H film on silicon substrate employing a D atom beam at a substrate temperature of 330 K. Experimental data are shown by solid circles. The solid and open squares represent model results. Point A corresponds to the beginning of the experiment. At point B (180 min later) the soft-layer formation is complete. Point C denotes the end of the experiment after 1200 min of D atom exposure.*

The goal of the simulations shown in Fig. 4 is to clarify the physical processes that take place while the ellipsometric angles change from point *A* to point *B* and a soft a-C:H layer is formed on the hard a-C:H film, and to obtain quantitative information on the thicknesses of the modified layer and the hard a-C:H film as a function of exposure time to D atoms. The physical information captured by the ellipsometry data can be revealed by comparison with the simulations. The overall finding is that the formation of a soft layer due to incorporation of D in the surface region of the a-C:H film takes place between points *A* and *B*. This phase is

accompanied by the onset of erosion and the erosion rate increases with time. Finally, between *B* and *C* the system shows steady-state erosion.

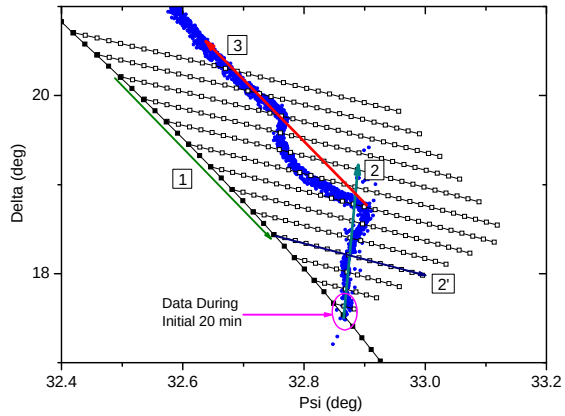

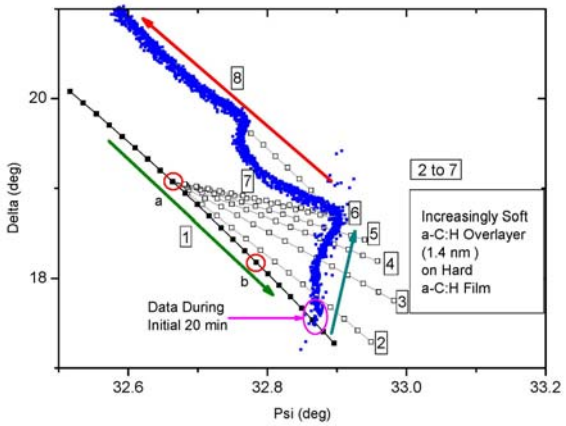

Fig. 4(b)

Figure 4: *(a) Ellipsometric map of hard a-C:H film (n=2.15, k=0.136) with soft a-C:H overlayer (n=1.57, k=0). Solid squares represent a hard a-C:H film with increasing thickness. Open squares represent soft a-C:H overlayers of increasing thickness on a hard film with varying thickness. The thickness difference between all model points corresponds to 0.1 nm. Experimental data obtained during deuteration of the hard a-C:H film employing a D atom beam are superimposed (solid circles). The intersection of the curve for the a-C:H film simulation and the experimental data corresponds to the initial film thickness of 74 nm. (b) Ellipsometric map of hard a-C:H film (n=2.15, k=0.136) (solid squares) on which 1.4 nm of increasingly soft a-C:H overlayers are produced (open squares). The refractive indices (n,k) for the different curves are: Curve 1 (n=2.15, k=0.136, i.e. the bulk material), curve 2 (n=1.99, k=0.04), curve 3 (n=1.81, k=0.02), curve 4 (n=1.7, k=0.007), curve 5 (n=1.59, k=0.0025), curve 6 (n=1.57, k=0.00) and curve 7 (n=1.55, k=0.00). Finally, curve 8 represents steady-state erosion of the hard a-C:H film (n=2.15, k=0.136) underneath an overlayer with constant 1.4 nm thickness and n=1.57, k=0.00). Experimental data obtained during deuteration of the hard a-C:H film employing a D atom beam are superimposed (solid circles). The model results 6 and 7 illustrate the conversion of a hard a-C:H film with a thickness of 0.7 nm (region between points a and b) into a 1.4 nm thick soft layer. Since point b corresponds to a total film thickness that is less than the initial film thickness (experimental data), about 0.5 nm material are eroded while the soft layer is completely established and steady-state erosion begins.*

The following considerations are helpful for the interpretation of the ellipsometric data in terms of physical processes. As D (or H) atoms are incident on the surface of the a-C:H material, replacement of H by D is followed by formation of additional C-D bonds in the near-surface region. The comparison of our hydrogenation and deuteration experiments has shown that the optical properties of a hydrogenated or deuterated a-C:H overlayer on top of a hard a-C:H film cannot be distinguished by ellipsometric measurements at 632.8 nm. Data to support this statement will be presented at the end of section III. Therefore, simple isotopic substitution of H atoms by D atoms that takes place during the initial D atom/a-C:H film interaction does not change the ellipsometric signal. This statement is consistent with the data of Fig. 3 for which the ellipsometry results obtained during the first 20 min show only little change from the hard a-C:H simulation (see the circled region near point *A*), but during which period the bulk of the D uptake of the sample occurs (see Fig. 2).

Conversion of the hard film into a soft, polymer-like layer with reduced refractive index *n* takes place as the D content of the modified layer builds up further. Only once additional C-D bonds are created, will the optical properties of the deuterated a-C:D_xH_y layer start to deviate from the optical constants of the hard a-C:H film. This change of the optical constants is not characteristic of the incorporation of deuterium, but the fact that the total hydrogen isotope content [hydrogen + deuterium atoms] increases and the mass density of the modified C:D_xH_y layer decreases simultaneously. A higher hydrogen isotope content and reduced density of the a-C:D_xH_y layer leads to a change of its optical properties such that the refractive index as well as the absorption decrease [25]. The temporal evolution of the reduction in atomic density and increasing H+D content of the a-C:D_xH_y layer can be followed by ellipsometry. From prior investigations we know that polymer-like films with $n = 1.57$, $k = 0$ have about half of the mass density of hard a-C:H films ($n = 2.15$, $k = 0.136$) [25]. Consequently, if we convert a certain thickness of a hard film into a soft film without mass loss, the soft film has about twice the thickness of the hard film. The uptake of additional deuterium leads to the conversion of a hard a-C:H film into a soft a-C:D_xH_y film with a greater thickness and can be obtained from the density ratio of the soft and hard a-C:D_xH_y films. In Fig. 4, we model this process of transformation as the growth of a soft a-C:D_xH_y layer on top of the hard a-C:H film for which the thickness is correspondingly reduced.

In the simulations, we examine two extreme cases. In the first we assume the formation of a soft a-C:D_xH_y layer with a constant refractive index (implying a fixed mass density and hydrogen + deuterium content) and a thickness that increases with time. This case is shown in Fig. 4(a). The other extreme is a situation where in-diffusion of D takes place within an a-C:H region extending a certain distance from the surface, and where the interaction with D atoms gradually reduces the atomic C density and increases the D + H content within this region. The extent of the modified region may be assumed to be equal to the thickness of the soft a-C:H layer that exists during steady-state erosion on the hard a-C:H film which was found from the simulation shown in Fig. 3 to be 1.4 nm in this work (corresponding to the displacement of curves 1 and 3 in Fig. 3). For the second model the optical properties of the modified layer are also assumed to be homogeneous throughout the layer but change continuously with time. The results of the corresponding simulations are shown in Fig. 4(b).

In Fig. 4(a), curve 1 (solid squares) corresponds to simulation results for a hard a-C:H film (n=2.15, k=0.136) of increasing thickness on a Si substrate (the separation of points in the direction of the arrow equals 0.1 nm thickness increase). The family of curves 2' (open squares) shows the effect of adding soft a-C:H overlayers (n=1.57, k=0) of increasing thickness on hard a-

C:H films with a given thickness. Each modeled line of the family of curves 2' correspond to a given constant thickness of the underlying hard a-C:H layer while the thickness of the soft a-C:H overlayer is increased. For the soft a-C:H layers, the separation of points in the arrow direction corresponds to 0.1 nm thickness increase. As we follow curve 2 in the direction of the arrow, each line 2' that is crossed corresponds to a soft a-C:H overlayer of increasing thickness grown on a proportionally thinner hard a-C:H film. A comparison of the ellipsometric map and the superimposed experimental data (solid circles) in Fig. 4(a) shows that there is a correspondence of the increase of the soft a-C:H overlayer and the thickness reduction of the hard a-C:H layer. However, if only transformation of a hard a-C:H layer into a soft a-C:D layer would take place, without loss of carbon atoms, the expected thickness of the soft overlayer would be twice the corresponding thickness of the converted hard a-C:H layer (this corresponds to the end of each of the curves 2') since the atomic density decreases correspondingly [25]. Instead, the comparison of the experimental data with the simulations shows approximately the same thickness for the converted hard a-C:H layer and the soft a-C:D layer that is formed. This shows that already some erosion must take place as hard a-C:H film is converted to produce a soft a-C:D layer. From the comparison of data and model we conclude that for the specific experimental conditions and a given thickness of hard a-C:H film that is either transformed into a soft a-C:D layer or eroded, about half of the carbon atoms from the original hard layer are present as a soft a-C:D layer and the other half are released in form of volatile species during the conversion process. This process continues until the thickness of the soft a-C:D layer no longer increases (point *B* in Fig. 3 is reached), and steady-state erosion commences (corresponding to the data between points *B* and *C* in Fig. 3). Figure 4 (a) shows nicely that simulations of soft a-C:D overlayers of fixed thickness on top of a hard a-C:H film with continuously decreasing thickness describes well this situation, and represents steady-state erosion of the hard a-C:H film.

The results of simulations addressing the second model are shown in Fig. 4(b). An ellipsometric map of a hard a-C:H film (n=2.15, k=0.136) on which 1.4 nm of increasingly soft a-C:H overlayers are modeled is shown. The spacing of the points for all simulations is 0.1 nm. The thickness of the hard a-C:H film on which 1.4 nm thick layers with various (n, k) combinations are simulated is constant. The refractive indices of the increasingly softer a-C:H films are based on measurements of both the H content, density and refractive indices of a-C:H layers deposited using a wide range of conditions similar to those described by Schwarz-Selinger et al. [25]. The refractive indices (n,k) for the different curves are: Curve 1 (n=2.15, k=0.136, = bulk material), curve 2 (n=1.99, k=0.04), curve 3 (n=1.81, k=0.02), curve 4 (n=1.7, k=0.007), curve 5 (n=1.59, k=0.0025), curve 6 (n=1.57, k=0.00) and curve 7 (n=1.55, k=0.00). Finally, curve 8 corresponds to steady-state erosion of the hard a-C:H film (n=2.15, k=0.136) underneath an overlayer with constant 1.4 nm thickness and n=1.57, k=0.00). The figure shows that as the a-C:H films become softer and of reduced mass density, the separation of points spaced 0.1 nm in the ellipsometric plane is reduced. The experimental data are superimposed on this map.

While different ways of comparing model and data are possible, the approach chosen here is to select point *B* of Fig. 3, when the behavior changes from the initial soft-layer formation (transient) to steady-state erosion. For curves 6 and 7 the model fits the data well, and marks the end of the transient phase. The model employed for curve 6, i.e. a hard a-C:H film with thickness *a* (circled point), on top of which 1.4 nm soft a-C:H is formed, can be used to describe the following steady-state erosion (curve 8) where the properties of the soft a-C:H layer remain the same. The comparison of actual data measured during the soft-layer formation stage with simulation results obtained employing a modified layer thickness of 1.4 nm and refractive

indices based on the different atomic densities of the surface layer shows discrepancies the between predictions of the simple model and actual data. These differences provide information on the physical processes taking place during the soft-layer build-up stage.

Using the atomic densities of the hard and soft carbon films, the starting thickness of the hard a-C:H layer would have to be located at point *b* (circled) to produce a final soft-layer thickness of 1.4 nm if no carbon loss would take place during the soft-layer build-up. This is the a-C:H thickness when steady-state erosion begins, and is 0.5 nm less than the actual a-C:H starting thickness (see the location within the area marked "data during initial 20 min", where measured data and hard a-C:H simulation (curve 1) intersect). Therefore, a corresponding number of carbon atoms is lost between the start of the experiment and the completion of the soft-layer formation. In other words, the comparison of experimental data and model predictions indicates that initially the thickness of the composite is reduced from the starting value, and that the modified layer formed has a thickness of less than 1.4 nm. This difference between experimental data and model is especially pronounced for curve 3, and indicates loss of a-C:H material during the experiment relative to the starting value of the hard a-C:H thickness. A hint of the expected thickness increase due to soft a-C:D layer formation expected for conditions where the total number of carbon atoms on the surface remains the same is possibly seen in the experimental data between curve 3 and curves 6 or 7. During this period the experimental data traverse the ellipsometric plane in a slightly different fashion as compared to the evolution between curves 1 and 3 (experimental data are initially parallel to ordinate axes, and then slope towards the right ordinate axis just before erosion commences).

The real-time ellipsometry data show that the soft-layer formation process is complete after about 180 min (corresponding to point *B* in Fig. 3), and is followed by steady-state erosion of the a-C:H film. This is represented by trajectory 8 parallel to curve 1 in Fig. 4(b). As noted before, during steady-state erosion the a-C:H film thickness decreases while a soft a-C:D_xH_y layer with approximately constant thickness remains on the hard a-C:H film.

Figures 3 and 4 show some additional details which we would like to comment on. The first is that the *complete temporal separation of isotopic exchange and soft layer formation is a simplification*. While the isotopic exchange is complete after about 20 min for our conditions (see Fig. 2, and also the more detailed evaluation described in section IV), some soft-layer formation has taken place at that point. This is indicated by the deviation of the ellipsometric data in direction of soft layer growth in Figs. 3 and 4. Secondly, we find that after the soft layer with a thickness of 1.4 nm has been established and steady-state erosion begun, a slight deviation of experimental data from curve 3 in Fig. 3 (or the corresponding curves in Figs. 4) is visible. While the reason for this change is not yet fully resolved, we attribute the deviations of the measured ellipsometry data from the model curve to experimental artefacts during this long-time experiment. Due to its high sensitivity, ellipsometry is very susceptible to changes of the sample temperature. Small changes of the sample temperature can be due to several reasons, one being a change of the laboratory temperature. We attribute the deviations of the data from the model curves in Figs. 3 and 4 to such changes of the sample temperature. The duration of the experiment was 20 h.

Comparison of the measured data of Fig. 4 with the simulations, consideration of the H content that corresponds to a particular refractive index, and the thickness of the modified layer enables us to determine the temporal dependencies of the modified ("soft") layer thickness, the transformed/removed "hard" layer thickness and of the steady state bulk erosion rate. These are presented next. In addition, the deuterium content of the modified ("soft") surface layer can be

obtained as a function of time, and this will be shown and discussed in section IV. From a practical view point, even though the model of Fig. 4 (b) may be physically more appealing, its evaluation is difficult since the refractive index of the modified surface region changes with time, and extraction of physical parameters requires information on the relationship of refractive index and soft-layer properties. The model of Fig. 4(a) uses a constant refractive index and variable thickness, and can be easily analyzed. All the data shown in the following are based on analysis of the experimental data using the simulations shown in Fig. 4(a). In part IV, we will compare extracted D areal density data for a few test cases obtained using the experimental data and the simulations shown in Fig. 4(b). These evaluations have shown that the two models produce results on extra D incorporation for given exposure times that agree with each other (see Fig. 11, where this comparison is shown).

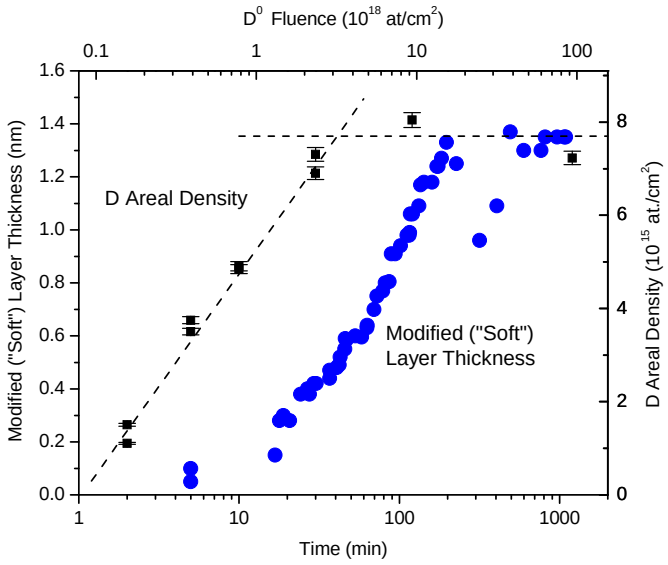

Figure 5: *Temporal evolution of the modified ("soft") layer thickness formed on a hard a-C:H layer during exposure to D atoms at a substrate temperature of 330 K versus exposure time or D atom fluence, respectively. The measured change in D areal density of the hard a-C:H layers as a result of exposure to D atoms is also shown.*

In Fig. 5 we combine key results of Fig. 2 and data obtained from analysis of Fig. 4(a). We compare the temporal evolution of the soft a-C:D_xH_y layer thickness formed on a hard a-C:H layer after a particular time of exposure to D atoms (obtained from the ellipsometric fitting of the experimental data) with the measured change of the D areal density. Here *Modified ("Soft") Layer Thickness* refers to the thickness of the surface layer that is characterized by a reduced refractive index. Figure 5 shows that most of the initial increase of the D areal density cannot be attributed to formation of the modified ("soft") layer. This indicates that transformation of C-H bonds to C-D bonds takes place more rapidly than formation of new C-D bonds. The first process is a simple isotopic exchange, whereas the second process corresponds to a change in the nature of the a-C:D_xH_y surface layer which alters its atomic density and hydrogen content and can be followed by ellipsometry due to the concomitant change of the optical constants of this layer. Figure 5 shows that some modified ("soft") layer thickness is produced prior to completion of the isotopic exchange in the surface layer, i.e. there is some temporal overlap of stages 1 and 2

in D atom/a-C:H film interaction. From a comparison of the ellipsometric data and the ion beam measurements we can conclude that the extra D incorporation that produces the soft a-C:D layer corresponds to a D areal density of ~2.5×10^{15} D cm^{-2} and occurs within ~1.4 nm from the surface.

In Fig. 6 we compare *Removed ("Hard") Layer Thickness*, i.e. the net thickness loss of the hard a-C:H layer observed during exposure to D atoms and explained by transformation and erosion, with the thickness of the soft a-C:D_xH_y layer formed on the hard a-C:H layer. We conclude that the bulk of the initial thickness loss of the hard a-C:H layer leads to formation of the soft a-C:D_xH_y layer. After about 180 min D atom exposure of the hard a-C:H layer, the thickness of the soft a-C:D_xH_y layer saturates, whereas the thickness loss of the hard a-C:H film continues. The inset in Fig. 6 shows that this thickness loss increases linearly with time. This is explained by steady state erosion of the hard a-C:H film.

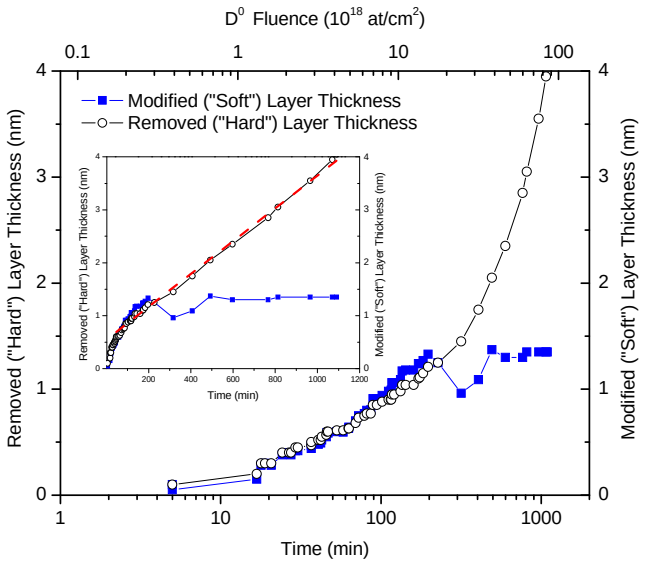

Figure 6: *The net thickness loss (transformation and erosion) of a hard a-C:H film during exposure to D atoms at a substrate temperature of 330 K versus exposure time or D atom fluence, respectively. The thickness of the soft a-C:D_xH_y layer formed on the hard a-C:H layer is also shown. The initial hard a-C:H layer thickness loss and the formation of the soft a-C:D_xH_y layer are closely related. After about 180 min, the thickness of the soft a-C:D_xH_y layer remains roughly constant, and steady state erosion of the hard a-C:H layer takes place. The inset shows the same data on a linear time scale and indicates that after about 180 min steady-state erosion of the hard layer prevails.*

As mentioned when discussing Figs. 4(a) and (b), a complete transformation of the *Removed ("Hard") Layer Thickness* into *Modified ("Soft") Layer Thickness* without simultaneous erosion would produce a soft layer that is twice as thick as the hard layer based on the differences in atomic density. Figure 6 shows instead that the two layers are nearly of the same thickness, indicating that roughly for each C atom that becomes part of a soft layer, another C atom is lost by erosion. This correspondence must be explained by the hydrogenation (deuteration) reaction of carbon atoms where for each C-C bond that is broken, two C-H (C-D)

bonds are formed. For a central C atom initially bonded to 4 carbon neighbors, this process can lead to CH_4 (CD_4) formation for the central C atom as simultaneously 4 C-H (C-D) bonds at the surrounding C atoms are established. In this case 4 C-D bonds become part of the a-C:D soft-layer, whereas the other 4 C-D bonds simultaneously formed lead to loss of one volatile carbon atom.

In Fig. 7 the net thickness loss of the hard a-C:H film during exposure to D atoms and the average rate at which the hard a-C:H layer thickness changes are shown as a function of D atom exposure time. It can be seen that during the initial period (first 60 min), when soft a-C:D_xH_y layer formation dominates, the average rate at which the hard a-C:H film thickness changes (solid squares) is at a maximum. The maximum is roughly four times the loss rate of the hard a-C:H film during the time regime when steady-state erosion of the hard a-C:H layer explains hard a-C:H loss, i.e. for times near 600 to 1000 min. A possible interpretation is that the soft layer formation rate provides a measure at which individual CD bonds are formed, whereas the average erosion rate of the a-C:H hard film is determined by the rate at which CD_4 is formed. Additionally, since erosion of a-C:H film requires that the material underneath the modified ("soft") surface layer is deuterated, the greater distance of the unmodified a-C:H material from the surface may play a role in the decrease of the average rate at which the hard a-C:H layer thickness changes.

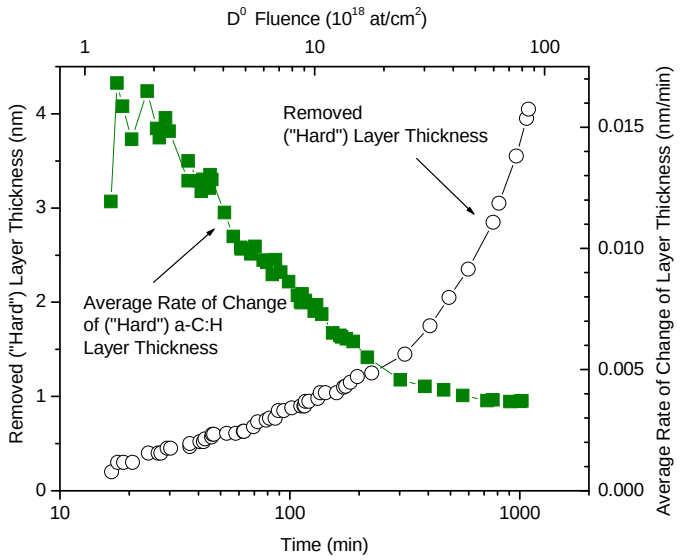

Figure 7: *Net thickness loss of hard a-C:H layer (open circles) during exposure to D atoms at a substrate temperature of 330 K versus exposure time or D atom fluence, respectively. The average rate at which the hard a-C:H film thickness changes (solid squares) is also shown. The maximum loss rate of the hard a-C:H film is seen during the period when the soft a-C:D_xH_y layer formation dominates, and is roughly four times the steady-state erosion rate of the hard a-C:H layer.*

A brief summary of the temporal sequence of processes is a follows: During the first 20 min of the experiment little change of the sample is seen by ellipsometry, and indicates that primarily isotope exchange takes place. Subsequently, conversion of increasing thickness of hard a-C:H film into a soft a-C:D_xH_y layer is seen. Since the isotope exchange reaction within the

modified layer is much faster than the addition of new deuterium atoms, we assume that all hydrogen in the modified layer has been exchanged by deuterium so that the hydrogen content in this layer is very small. Figure 4(b) shows that the thickness of the modified layer during this period is less than the final thickness (1.4 nm) reached when steady-state erosion commences. This phase is accompanied by the onset of chemical erosion [15], i.e., formation of volatile hydrocarbon species that leave the surface. The chemical erosion rate increases with time. At the end of this phase, when chemical erosion has reached its steady-state value about half of the carbon being originally present in the hard film that was converted has been eroded. This is followed by steady-state erosion after about 180 min, where a modified layer of about 1.4 nm remains on the surface. Chemical erosion is very inefficient at the temperature of the experiment (330 K) and has been described by Schlüter et al. [28].

Erosion at Elevated Temperatures Using D or H Atoms. A similar sequence of processes as described for a substrate temperature of ~330 K takes place at elevated substrate temperature, though at a much faster rate. This is shown in Fig. 8, where we show ellipsometry data obtained during exposure of a roughly 70 nm hard a-C:H film using a D atom beam at a substrate temperature of 650 K. The sample had been preheated to 650 K for 1 h before exposure to the D atom flux. The total length of D atom exposure time was 140 min. Figure 8 shows along with the experimental data an ellipsometric map obtained by simulating a hard a-C:H film (n=2.16, k=0.15) of variable thickness (curve 1). Additionally, Fig. 8 shows simulation curves that correspond to a hard a-C:H film (n=2.16, k=0.15) of variable thickness covered with a soft a-C:H overlayer (n=1.57, k=0) of 1, 2, 3, 4 or 5 nm thickness, respectively. During the first 600 s of D atom exposure, the experimental data show primarily the formation of a 2 nm thick soft layer on top of the hard a-C:H film, along with loss of carbon atoms. This is clearly seen in the inset, where the experimental data initially follow a trajectory parallel to curve 2 and perpendicular to curve 1, and cross the line corresponding to 2 nm soft a-C:H after 600 s of exposure to the D atom beam. The soft layer formation is greatly accelerated at 650 K relative to 330 K, and the thickness of the soft layer is also greater at the elevated temperature. After 600 s, steady-state erosion dominates the response. During erosion, the soft layer thickness increases slowly, while the hard a-C:H layer thickness decreases fairly rapidly. Possible reasons for the non-idealities seen in Fig. 8 along the erosion curve 3 may be a variation of the initial a-C:H film properties with film thickness, and possibly formation of surface roughness during the significant a-C:H film erosion that takes place during this experiment. Chemical erosion of a-C:H films due to exposure of hydrogen atoms as a function of temperature has been thoroughly investigated by Schlüter et al. [28].

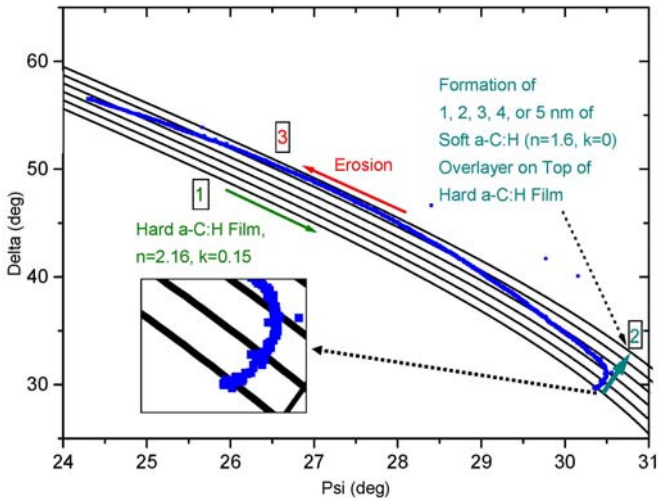

Fig. 8

Figure 8: *Ellipsometry data obtained during erosion of hard a-C:H film using D atom beam at a substrate temperature of 650 K. The data are superimposed on ellipsometric maps (solid lines) showing a hard a-C:H film (n=2.16, k=0.15) with soft a-C:D_xH_y overlayer (n=1.57, k=0) of 1, 2, 3, 4 and 5 nm thickness, respectively. During the first 600 s of D atom exposure a 2 nm thick soft layer is formed. This is followed by steady-state erosion and a thickness increase of the soft a-C:D_vH_v overlaver.*

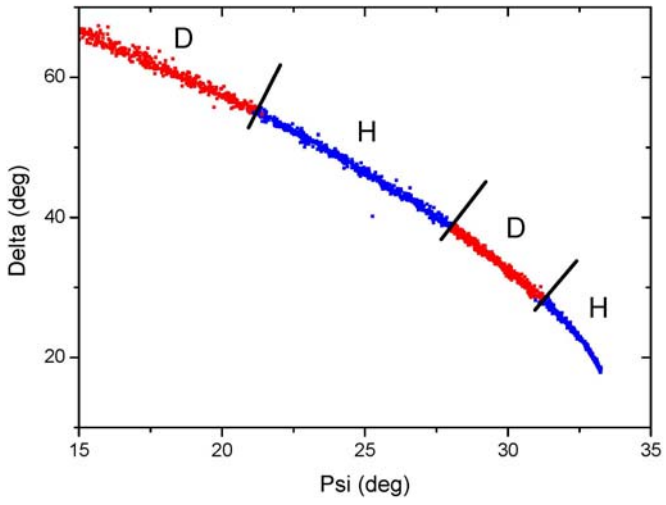

Fig. 9

Figure 9: *Ellipsometric trajectory for hard a-C:H film exposed sequentially to H atoms, D atoms, H atoms, and D atoms at a substrate temperature of 650 K. The deuterated or hydrogenated soft layer formed on top of the hard a-C:H film during D atom or H atom exposures, respectively, cannot be distinguished by ellipsometry at 632.8 nm.*

In Fig. 9 real time ellipsometry data obtained during erosion of a hard a-C:H film at 650 K by exposure to H atoms, then D atoms, followed by H atoms and finally D atoms for a total exposure time of more than 280 min are shown. The key information that can be read from Fig. 9 is that the shape of the ellipsometric trajectory measured is independent if H or D are used for erosion. This indicates that the formation of soft a-C:D/a-C:H layers produced by D/H atom

exposure from a-C:H layers for the conditions employed in the present work, did not produce measurable differences in the optical properties of these layers if ellipsometry at 632.8 nm is used for characterization.

While H atom beam exposures of a-C:D or a-C:H layers were only of secondary interest in this work, we observed that measured steady-state a-C:H erosion rates were about 30% greater for H atom than for D atom exposures at 650°C for otherwise comparable conditions. This could be concluded from detailed ellipsometric simulation of the data shown in Fig. 9, was also reproduced in other experiments. The identification of the cause(s)s of this difference is not straightforward, since the actual H atom flux at the substrate is not well-known for the present experiments. We confirmed that the H_2 flow through a cold capillary was about 40 % greater than the D_2 flow for the experimental conditions used here (same inlet gas pressure). We also verified that the angular dependence of the H and D atom flux distributions were identical by comparing three-dimensional erosion profiles for H and D atoms produced in a-C:H films patterns and employing a movable mass spectrometer. While differences in H_2 and D_2 gas flow are a likely reason for the observed erosion rate differences, the contributions of changes in the D_2 and H_2 degree of dissociation and kinetic isotope effect (rate of carbon attack by H or D atoms reflects the reduced mass of C-H or C-D [37,38]) has not been clarified. Additional work is required to elucidate the mechanistic origin of this observation.

IV. Discussion

A. Isotope Exchange, Soft Layer Formation and Erosion

Figure 10 displays a schematic picture showing the three stages of D atom interaction with a hard a-C:H layer at a substrate temperature of 330 K revealed in the present work. The first step is hydrogen replacement of the a-C:H film at an areal density of roughly 5×10^{15} D cm^{-2} (Fig. 10(a)). The hydrogen replacement is a two step process [19]. Impinging D abstracts bonded H from the film with a cross section of about 0.05×10^{-16} cm^2 [19] forming HD and leaving behind a dangling bond at/or near the surface. The next impinging D atom on this dangling bond site is then bonded to the film. The cross section for H or D addition to a dangling bond site is about 4.5×10^{-16} cm^2 [19]. This isotope exchange process in the near surface layer is complete after ~ 20 min for our experimental conditions, and corresponds to an impinging D fluence of about 2×10^{18} cm^{-2}. The next phase is dominated by creation of additional C-D bonds at an areal density of ~ 2.5×10^{15} D cm^{-2} which transforms the hard carbon layer into a soft a-C:D layer that extends ~ 1.4 nm from the surface (see Fig. 10(b)). Some carbon erosion takes place simultaneously. As discussed above, a definite relationship between the number of extra C-D bonds formed and the number of C-atoms eroded is observed and expected. This process is complete after ~ 180 min (about 1.4×10^{19} D cm^{-2}), and is followed by steady-state erosion of the a-C:H film. Erosion is plausible, since upon injection of D into the surface region, volatile CD_z is produced once the D density in the surface layer rises above a critical value (presumably CD_4), and a net thickness loss of the composite layer structure is seen (Fig. 10(c)). As steady-state erosion of the a-C:H layer takes place, the soft a-C:D_xH_y layer is dynamically reformed at the

interface of the original hard a-C:H layer and the modified surface layer. A roughly constant thickness of the soft overlayer is maintained during the steady-state erosion process.

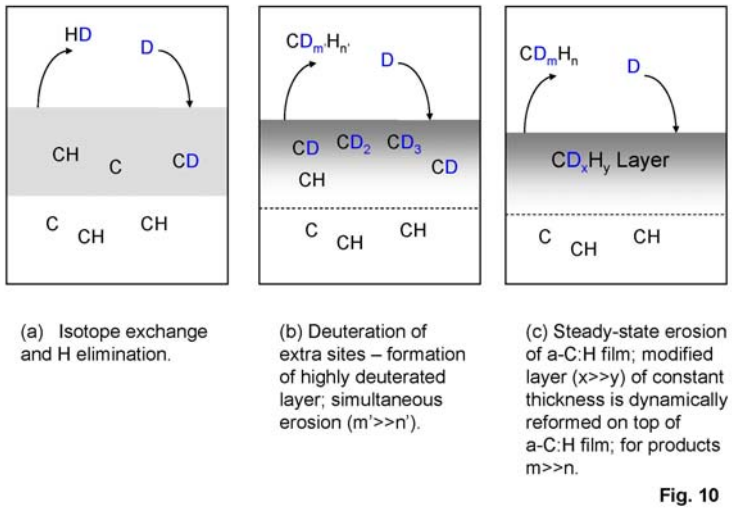

Figure 10: Schematic picture showing three stages of D atom interaction with hard a-C:H layer on Si substrate at a substrate temperature of 330 K.

B. Cross Section for Isotope Exchange

For the experiments described here, the D atom flux, the absolute change in D areal density at the surface, along with the thickness of the layers are known (the quantification of the D atom flux described by Schwarz-Selinger et al. [27] was performed for D). This allows modeling the data quantitatively and extracting fundamental interaction parameters. For simple isotope exchange in a-C:H films the density of deuterated carbon-hydrogen bonds satisfies

$$n_D(t) = n_H(0) - n_H(t) \qquad (1)$$

where $n_D(t)$, $n_H(t)$ and $n_H(0)$ are the number densities of deuterated or hydrogenated bonds at time t or $t=0$, respectively. We write the time rate of change of $n_H(t)$ as

$$\frac{dn_H(t)}{dt} = -n_H(t)\sigma\Phi\,, \qquad (2)$$

where σ is the cross section for hydrogen-deuterium exchange, and Φ the flux of deuterium atoms (1.3×10^{15} D cm^{-2} s^{-1}). The hydrogenated bonds n_H are located within a certain distance from the surface (~1.4 nm). In this near-surface layer, deuterium exchange takes place (see Fig. 10(a)). Integration of equation (2) and solving for $n_D(t)$ yields

$$n_D(t) = n_H(0)\left[1 - \exp\left(-t\sigma\Phi\right)\right]. \qquad (3)$$

We used equation (3) to extract the cross section σ for hydrogen-deuterium exchange from the experimental data. From the change of the deuterium areal density measured during the first

2 min or 5 min deuterium atom exposure, when deuterium exchange dominates the change in D areal density, we find $\sigma = 2.0\times10^{-18}$ cm^2. If data obtained for longer exposure times were used for the fit, soft layer formation could contribute to the measured D areal density and change the values of the cross section obtained, i.e. an apparent $\sigma = 1.2\times10^{-18}$ cm^2 is found for 10 min exposure time.
Comparison of this cross-section with results of cross-section measurements described in the literature for H-atom interactions with carbon surface layers shows that this corresponds closely to the measured cross-section of hydrogen abstraction from a graphite surface ($\sigma = 5\times10^{-18}$ cm^2, see Ref. [19]). In view of the relatively large uncertainties associated with the determination of the values for σ the agreement between these two values has to be considered satisfactory. An interpretation of this result is that isotope exchange is limited by the elimination of H from the a-C:H surface by HD product formation (see Fig. 10 (a)).

In Fig. 11 we show the data of Fig. 2, along with three extra data sets based on additional analysis of the data. The solid line corresponds to equation (3) with $\sigma=2.0\times10^{-18}$ cm^{-2}, a flux $\Phi = 1.3\times10^{15}$ D cm^{-2} s^{-1}, and $n_H(0)= 5.0\times10^{15}$ cm^{-2} (the value of $n_H(0)$ is based on Fig. 2). The expression is in agreement with the change in D areal density measured during H exposure of a-C:D films (solid diamonds), which presumably only measures the loss of D due to isotope exchange. The comparison with the total change in D areal density (solid squares) shows that the initial sample modification is dominated by isotope exchange. This isotope exchange is complete after about 20 min.

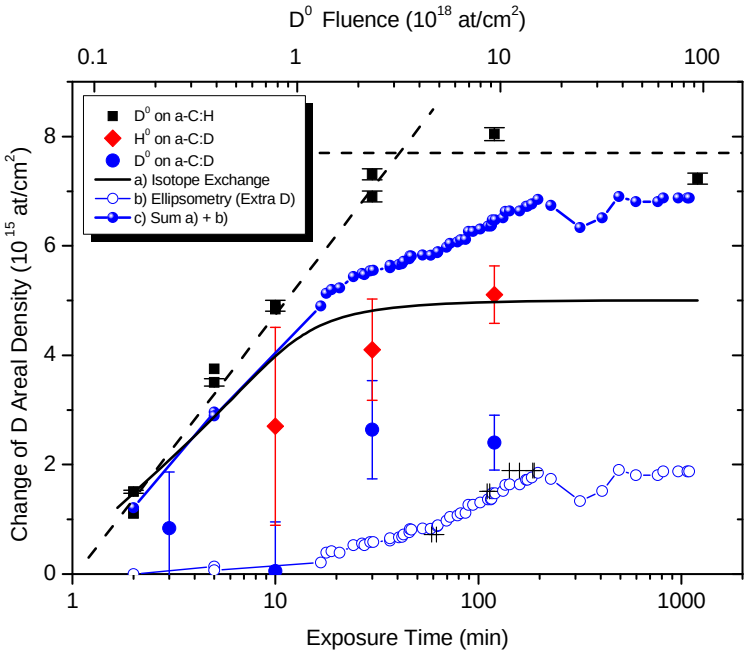

Figure 11:. Comparison of D areal density data from figure 2 with a) D areal density due to isotope exchange (equation (3)), and b) extra D incorporation in surface region obtained from soft a-CD_xH_y layer formation monitored by ellipsometry. The data c) correspond to the sum of a) and b). The substrate temperature is 330 K and exposure time is converted into fluence by using a flux $\Phi = 1.3\times10^{15}$ at/cm^2 s for the D atom exposures. The actual fluence may be higher for the H atom exposures. Curve b) shows a comparison of the extra D obtained from analysis using either the model of Fig. 4(a) (circles) or Fig. 4(b) (+ symbols).

Figure 11 shows the extra D areal density that can be extracted from the kinetics of soft-layer formation obtained by analysis of the ellipsometric data (open circles). For this we employ the thickness and refractive index of the soft a-C:D layer that is formed, and use the relationship between refractive index and D (H) content of the hydrocarbon layer [25]. We also take into account the thickness increase of the initial hard a-C:H layer as it is modified into a soft a-C:D layer and subtract its initial H content (obtained from $n_H(0)$, since the H atoms in the as-deposited layer will be replaced by D atoms, and the isotopic substitution will not be reflected in the ellipsometric analysis). Figure 11 shows that the areal density of extra D found in this way (open circles) is in reasonable agreement with the change in D areal density measured during D exposure of a-C:D films (solid circles) (except for the data point measured after 30 minutes exposure).

Several extra D areal density values obtained by the method used for Fig. 4(b) are displayed as "+"-symbols. The data shown are in reasonable agreement with the data obtained using the model shown in Fig. 4(a).

Figure 11 also shows the sum of the change in D areal density as given by the model of isotope exchange (equation 3) and the extra D due to soft a-C:D layer formation measured by ellipsometry (connected dots). These data compare reasonably well with the total change in D areal density measured during D exposure of a-C:H films (solid squares), confirming the general consistency of the picture presented in Fig. 10.

The D areal densities measured by IBA are absolute and no model of the surface region is required for the interpretation of the data. A reasonable first approximation is to assume that the sample depth for which deuterium exchange takes place and the layer thickness that is transformed into a soft a-C:D film are the same. The fact that an initial areal density $n_H(0) = 5.0\times10^{15}$ cm^{-2} - experimentally measured - can explain the deuterium exchange component indicates that isotope exchange affects an a-C:H film thickness that is slightly greater than that which is transformed into a soft layer (the number of H atoms in 1 nm of hard a-C:H film – more than required to produce 1.4 nm of soft film if the expansion due to the density change is taken into account - corresponds to 4.0×10^{15} cm^{-2}). This difference is reasonable, since in general, the assumption of a homogeneous layer of uniform composition used for the analysis of the ellipsometry data is likely too simple, and layers with a graded composition may provide a better description of the actual physical situation.

C. Relationship to Other Work

Boutard et al. [39,40,41] performed studies of isotopic exchange of H and D in hard a-C:H and a-C:D films as a result of ion bombardment of the films with protons and deuterons. In their work the incident ion energy played an important role in the isotopic replacement, and the resulting deuterium or hydrogen levels. The situation studied in the present work is significantly different and must be analyzed in a different fashion.

Küppers and coworkers [19,42,43] developed a detailed model of hydrogen-atom induced chemical erosion of carbon films based on surface science studies. In their work carbon layers of only a few monolayers thickness were studied, and steady-state erosion similar to that studied in the present work was not achieved. Our work shows that chemical erosion of carbon films by D or H atoms is not a simple surface chemistry mechanism, but takes place in an extended near-surface region. Before any significant erosion occurs, a deuterium-rich (hydrogen-

rich) modified surface layer is formed, with a thickness of several nm. The volatile products are formed in this dynamic layer which is constantly reformed as steady-state erosion proceeds.

Investigating the influence of a–C:H films on the gas and plasma driven permeation of hydrogen through iron foils, Pillath et al. [44] concluded that atomic hydrogen can penetrate about 2 nm deep into a–C:H films. This thickness is in good agreement with the penetration depth of 1.4 nm obtained in this work.

Keudell and co-workers [16,17] investigated the erosion of a–C:H films in hydrogen plasmas by real-time ellipsometry. They found that the interaction of low-energetic hydrogen species, i.e. atomic hydrogen and H ions with energies below 20 eV from the plasma, cause a hydrogenation of the a–C:H film surface. They estimated a thickness of about 1 nm for this modified layer which is also in agreement with the data presented in this article.

V. Conclusions

We have studied the interaction of hard a-C:H (a-C:D) layers at a substrate temperature of 330 and 650 K with a quantified D-atom beam. Ion beam measurements of the D areal density change as a function of D fluence coupled with results of real-time ellipsometry data provide a consistent picture of three essentially sequential physical processes that take place as a function of fluence. At a substrate temperature of 330 K, hydrogen replacement by deuterium at an areal density of $\sim 5\times10^{15}$ D cm^{-2} is followed by creation of additional C-D bonds to a depth of ~1.4 nm from the surface and adds an extra D areal density of $\sim 2.5\times10^{15}$ D cm^{-2}. The study of this process is based on interpretation of ellipsometry data showing the formation of a soft a-C:D layer on top of the hard a-C:H layer. Subsequently, steady-state erosion of the a-C:H film takes place, where the soft a-C:D layer with roughly constant thickness remains on the underlying hard a-C:H film. The magnitude of the cross section for the D-H isotope exchange in the a-C:H film ($\sigma=2.0\times10^{-18}$ cm^2) is close to that of H-H abstraction from a carbon surface, and corroborates the assumption that H abstraction by D from the a-C:H surface is a rate limiting step for this process.

Acknowledgments. We thank T. Dürbeck for technical assistance, and Drs. U. von Toussaint and Ch. Hopf for helpful discussion. GSO would like to thank Prof. Bolt and the Materials Research Division at the Max-Planck Institut für Plasmaphysik (IPP), Garching, Germany, for their hospitality, and University of Maryland for support of this sabbatical period.

References

[1] A. Bubenzer, B. Dischler, G. Brandt, and P. Koidl, Journal of Applied Physics **54**, 4590 (1983).
[2] J. Robertson, Materials Science & Engineering R-Reports **37**, 129 (2002).
[3] M. Meyyappan, L. Delzeit, A. Cassell, and D. Hash, Plasma Sources Science & Technology **12**, 205 (2003).
[4] M. Terrones, International Materials Reviews **49**, 325 (2004).
[5] V.I. Merkulov, A.V. Melechko, M.A. Guillorn, D.H. Lowndes, and M.L. Simpson, Applied Physics Letters **79**, 2970 (2001).
[6] H. Yasuda, *Plasma Polymerization*, (San Diego, Academic Press, 1985).
[7] *Plasma Processes and Polymers*, edited by R. d'Agostino, P. Favia, C. Oehr, and M. R. Wertheimer, (Berlin, Wiley-VCH, 2005).
[8] J. Behnisch, A. Hollander, and H. Zimmermann, Journal of Applied Polymer Science **49**, 117 (1993).
[9] N. Inagaki, S. Tasaka, and T. Umehara, Journal of Applied Polymer Science **71**, 2191 (1999).
[10] S. Vasquez-Borucki, C. A. Achete, and W. Jacob, Surface & Coatings Technology **138**, 256 (2001).
[11] P. Kruger, R. Knes, and J. Friedrich, Surface & Coatings Technology **112**, 240 (1999).
[12] O. Louveau, C. Bourlot, A. Marfoure, I. Kalinovski, J. Su, G. Hills, and D. Louis, Microelectronic Engineering **73-74**, 351 (2004).
[13] G. J. Stueber, G. S. Oehrlein, P. Lazzeri, M. Bersani, M. Anderle, R. McGowan, and E. Busch, J. Vac. Sci. Technol. B **25**, 1593 (2007).
[14] J. Opretzka, J. Benedikt, P. Awakowicz, J. Wunderlich, and A. von Keudell, Journal of Physics D-Applied Physics **40** (9), 2826 (2007).
[15] W. Jacob and J. Roth, "Chemical Sputtering", in: *Sputtering by Particle Bombardment, Experiments and Computer Calculations from Threshold to MeV Energies*, R. Behrisch and W. Eckstein (Eds.) Springer, Berlin 2007, pp. 329 – 400.
[16] A. von Keudell and W. Jacob, Journal of Applied Physics **79**, 1092 (1996).
[17] A. von Keudell and W. Jacob, Journal of Vacuum Science and Technology **A 15**, 402 (1997).
[18] W. Jacob, Thin Solid Films **326**, 1 (1998).
[19] J. Küppers, Surface Science Reports, **22**, 251 (1995).
[20] G. Federici, J. N. Brooks, D. P. Coster, G. Janeschitz, A. Kukuskhin, A. Loarte, H. D. Pacher, J. Stober, and C. H. Wu, Journal of Nuclear Materials **290**, 260 (2001).
[21] J. Roth, Physica Scripta **T124**, 37-43 (2006).
[22] C. H. Skinner and G. Federici, Physica Scripta **T124**, 18 (2006).
[23] W. Jacob J. Nucl. Mater. **337–339**, 839 (2005).
[24] E. Vietzke and V. Philipps, Fusion Technology **15**, 108 (1989).
[25] T. Schwarz-Selinger, A. von Keudell, and W. Jacob, Journal of Applied Physics, **86**, 3988 (1999).
[26] W. Jacob, C. Hopf, A. von Keudell, M. Meier, and T. Schwarz-Selinger, Review of Scientific Instruments **74**, 5123 (2003).
[27] T. Schwarz-Selinger, A. von Keudell, and W. Jacob, J. Vac. Sci. Technol. A **18**, 995 (2000).

[28] M. Schlüter, C. Hopf, T. Schwarz-Selinger, and W. Jacob, J. Nucl. Mater. **376**, 33 (2008).
[29] B. Landkammer, A. von Keudell, and W. Jacob, J. Nucl. Mater. **264**, 48 (1999).
[30] V. Kh. Alimov, M. Mayer, and J. Roth, Nucl. Instr. Meth. B **234**, 169 (2005).
[31] M. Mayer, "SIMNRA User's Guide", Report IPP 9/113, Max-Planck-Institut für
249 Plasmaphysik, Garching, Germany (1997)
[32] David R. Lide., CRC Handbook of Chemistry and Physics (2005).
[33] R. L. Bruce, S. Engelmann, T. Lin, T. Kwon, R. Phaneuf, G. S. Oehrlein, B. K. Long, C. G. Willson, J. J. Végh, D. Nest, D. B. Graves, and A. Alizadeh, J. Vac. Sci. & Technol. **B 27,** 1142 (2009)**.**
[34] F. Weilnboeck, N. Fox-Lyon, G S Oehrlein, and R. P. Doerner, Nucl. Fusion **50**, 025027 (2010).
[35] S. Engelmann, R. Bruce, T. Kwon, R. Phaneuf, G. S. Oehrlein, Y. C. Bae, C. Andes, D. Graves, D. Nest, E. A. Hudson, P. Lazzeri, E. Iacob and M. Anderle, J. Vac. Sci. & Technol. **B 25**, 1353 (2007).
[36] R. L. Bruce, F. Weilnboeck, T. Lin, R. J. Phaneuf, G. S. Oehrlein, B. K. Long, C. G. Willson, J. J. Végh, D. Nest and D. B. Graves, Journal of Applied Physics, 107, 084310 (2010).
[37] K. B. Wiberg, Chem. Revs., **55**, 713 (1955).
[38] F. H. Westheimer, Chem. Revs., **61**, 265 (1961).
[39] D. Boutard, W. Moller, and B. M. U. Scherzer, Journal of Applied Physics, **67**, 163 (1990).
[40] D. Boutard and W. Moller, Journal of Materials Research, **5**, 2451 (1990).
[41] D. Boutard, W. Moller, and B. M. U. Scherzer, Radiation Effects and Defects in Solids, **114**, 281 (1990).
[42] T. Zecho, B. D. Brandner, J. Biener, and J. Küppers, Journal of Physical Chemistry B, **105**, 6194 (2001).
[43] T. Zecho, A. Guttler, X. W. Sha, B. Jackson, and J. Küppers, Journal of Chemical Physics, **117**, 8486 (2002).
[44] J. Pillath, J. Winter and F. Waelbroek, in: *Amorphous hydrogenated carbon films*, P. Koidl and P. Oelhafen (eds), E-MRS Symposia Proc., Vol. XVII, 449, Les Ulis, Les Editions de Physique, 1987.